NASA TECHNICAL MEMORANDUM

NASA TM-82517

ATTITUDE CONTROL AND DRAG COMPENSATION PROPULSION SYSTEM FOR THE GRAVITY PROBE-B SPACECRAFT

By D. H. Blount

Structures and Propulsion Laboratory
Science and Engineering Directorate

January 1983

NASA

George C. Marshall Space Flight Center
Marshall Space Flight Center, Alabama

TECHNICAL REPORT STANDARD TITLE PAGE

1. REPORT NO.	2. GOVERNMENT ACCESSION NO.	3. RECIPIENT'S CATALOG NO.
NASA TM-82517		

4. TITLE AND SUBTITLE	5. REPORT DATE
Attitude Control and Drag Compensation Propulsion System for the Gravity Probe-B Spacecraft	January 1983
	6. PERFORMING ORGANIZATION CODE
7. AUTHOR(S)	8. PERFORMING ORGANIZATION REPORT #
D. H. Blount	
9. PERFORMING ORGANIZATION NAME AND ADDRESS	10. WORK UNIT NO.
George C. Marshall Space Flight Center Marshall Space Flight Center, Alabama 35812	11. CONTRACT OR GRANT NO.
	13. TYPE OF REPORT & PERIOD COVERED
12. SPONSORING AGENCY NAME AND ADDRESS	Technical Memorandum
National Aeronautics and Space Administration Washington, D.C. 20546	14. SPONSORING AGENCY CODE

15. SUPPLEMENTARY NOTES

Prepared by Structures and Propulsion Laboratory, Science and Engineering Directorate.

16. ABSTRACT

An on-board propulsion system for attitude control and drag compensation is presented which uses helium boiloff gas from an experiment package dewar as propellant. This boiloff gas would normally be vented non-propulsively. Use of a small allowable temperature range in the dewar is exploited to store helium and accommodate incompatibilities in dewar heat leak and thruster demand flow over periods of more than one orbit. A relatively detailed thermodynamics analysis of the two-phase helium dewar and simulation of pressure loss through the helium distribution system is included.

17. KEY WORDS	18. DISTRIBUTION STATEMENT
	Unclassified – Unlimited

19. SECURITY CLASSIF. (of this report)	20. SECURITY CLASSIF. (of this page)	21. NO. OF PAGES	22. PRICE
Unclassified	Unclassified	37	NTIS

TABLE OF CONTENTS

LIST OF ILLUSTRATIONS

DEFINITION OF SYMBOLS

Q	Heat
W	Work
V	Volume
P	Pressure
M	Mass
$\dot{W}$	Mass flow rate
q	Heat transfer per unit time
U	Internal energy
u	Specific internal energy
h	Specific enthalpy
t	Time
v	Specific volume
ρ	Density
T	Temperature
$f(\ )$	Function of (given variable)
R	Gas constant; flow resistance
C	Constants in curve fits
C_p	Specific heat at constant pressure
D	Constant in curve fit; hydraulic diameter
c	Constants in curve fits
$CONV_1$	Conversion constant
L	Length
A	Area
g_c	Dimensional constant

N_{Re}	Reynold's number
μ	viscosity
K	Flow resistance factor
Subscripts	
V	Saturated vapor
L	Saturated liquid
fg	Difference between property of saturated liquid and saturated vapor at the same temperature and pressure
D	Total dewar
i	Initial state
T	Total
B	Base or starting point
P	Thruster supply delivery point; porous plug
CRIT	Porous plug critical flow rate point
O	Nominal reference point
C	Contraction
E	Expansion
X	Cross sectional
h	Hydraulic
R	Cooling ring
L	Line
SR	Support Ring

TECHNICAL MEMORANDUM

ATTITUDE CONTROL AND DRAG COMPENSATION PROPULSION SYSTEM FOR THE GRAVITY PROBE-B SPACECRAFT

I. INTRODUCTION

The on-board propulsion system for the Gravity Probe-B spacecraft must provide attitude control plus thrust to effectively cancel the atmospheric drag encountered at the relatively low orbit dictated by current shuttle capability. A propulsion system was desired which would utilize the boiloff of helium gas from the experiment package dewar as propellant. This helium boiloff would normally be vented non-propulsively and, thus, in a sense be "wasted." A system was devised which could reconcile the thrust requirements and the available helium boiloff to provide 100 percent drag free control of the vehicle.

Derivation of the necessary thermodynamic equations is shown and a computer code for a relatively rigorous simulation of the two-phase helium dewar is provided along with details of the delivery line pressure loss calculation. These mathematical models were used to estimate the dewar pressure and temperature as a function of time during the predicted extremes of thruster demand and dewar heat absorption.

II. SYSTEM REQUIREMENTS AND DESIGN FACTORS

The requirements for the propulsion system were established by the need to provide precise attitude control and to provide an additional thrust vector to effectively cancel the vehicle drag incurred by the spacecraft. The thrusters are paired back-to-back with clusters of two pairs located at the ends of the four solar array spars for a total of 16 individual thrusters. Their location relative to the vehicle is illustrated in Figure 1. Each of the thrusters consists of a flow control valve and nozzle and is required to produce a maximum thrust of 650 dynes with a thrust tolerance of ±2 percent of the open loop commanded value. The desired transient response of the thruster to a step input thrust command is that of an underdamped second-order system

$$F/F_{COM} = 1 + \frac{e^{-\zeta\omega_n t}}{\sqrt{1+\zeta^2}} \sin\left(\omega_n\ t\sqrt{1-\zeta^2} - \alpha\right)$$

where

$\alpha = \cos^{-1}(-\zeta)$ in radians

t = time in sec

F = delivered thrust

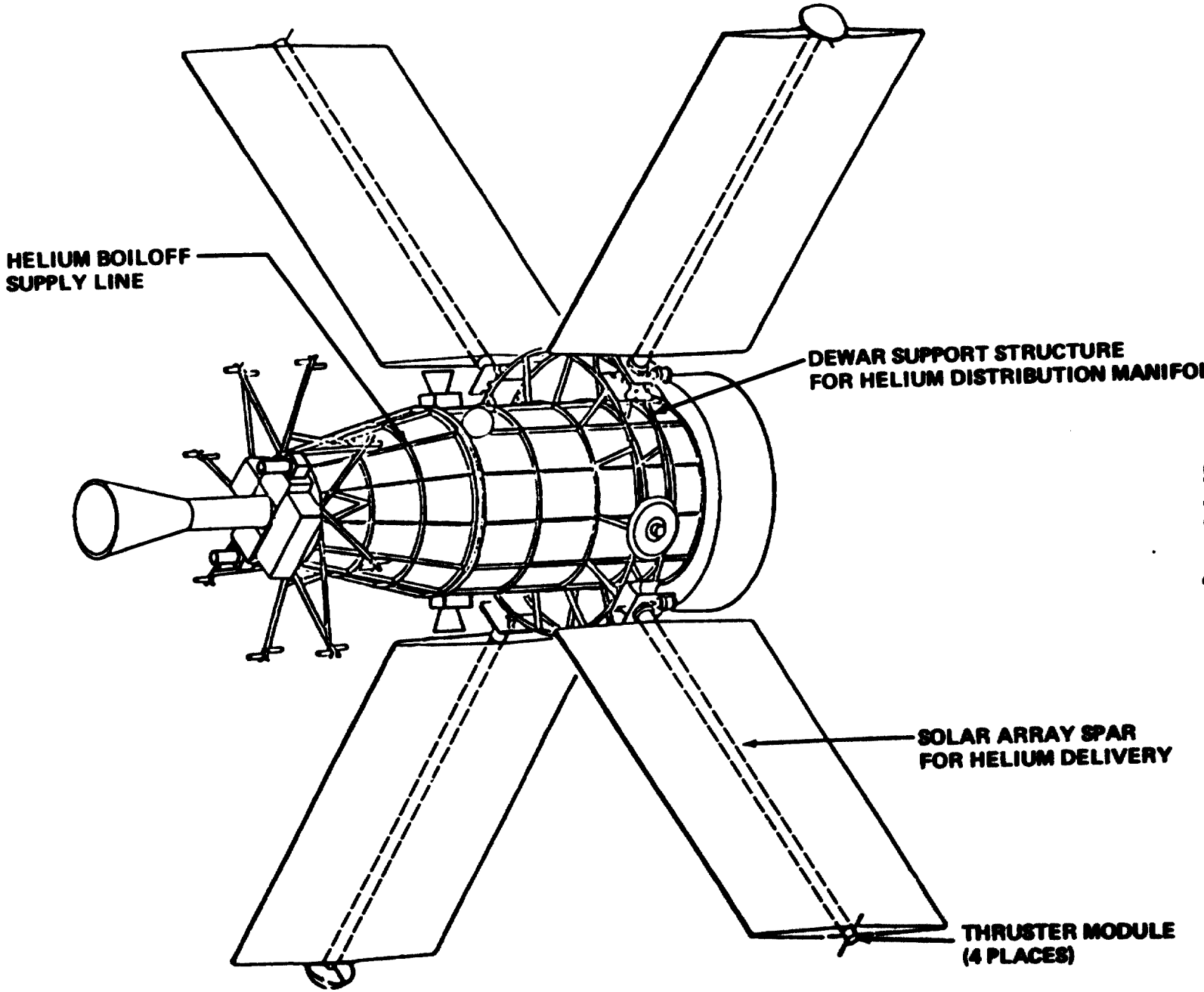

Figure 1. Gravity Probe-B Spacecraft attitude control system.

F_{com} = command thrust

ω_n = undamped natural frequency radians/sec

ζ = damping factor

with the values of natural frequency, ω_n, and damping factor, ζ, set at 10 Hz (62.8 RAD/sec) and 0.707 respectively.

The thruster flow control valve is required to respond to thrust command changes as small as 0.1 dynes in the closed loop mode. This very small thrust tolerance is necessary to maintain the vehicle within the acceleration limit of 10^{-10} g (this assumes two thrusters are operating together for drag makeup).

The maximum total thrust required at any one time is set at 1300 dynes. Although this thrust happens to be equal to twice the maximum thrust of two nozzles, as many as eight thrusters could be operating simultaneously at less than their maximum values. This maximum thrust is set by the maximum atmospheric density expected during a 90 min orbit. The required thrust will statistically vary as shown in Figure 2.

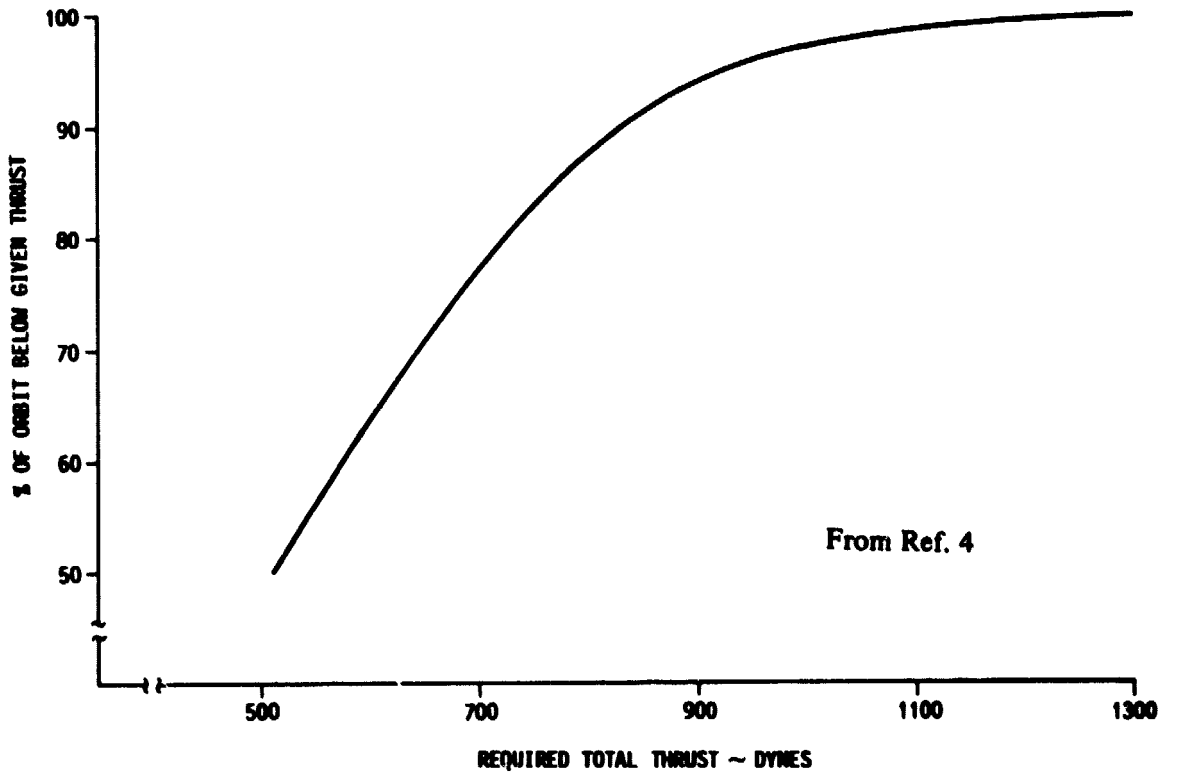

Figure 2. Orbital variation of required total thrust.

The constraints within which the helium boiloff thruster system must operate are set by the experiment package dewar design, the 1 year life requirement, and the solar heat pickup capability of the helium delivery lines. The heat leak into the dewar (which contains an initial 300 kg load of helium in a saturated liquid form) is expected to range from a low of 0.1849 to a high of 0.2326 W. A nominal dewar temperature of 1.6°K with an allowable tolerance of ±0.1°K was considered satisfactory to provide the superfluid helium II conditions required by the experiment package. The solar heat picked up by the boiloff helium as it cools the dewar thermal shields and traverses the lines leading to the thruster modules at the ends of the solar array spars raises its temperature to between 300° and 375°K. Finally, the vehicle solar array and power supply system indicate a power/weight penalty of 1.5 kg/W. These requirements are summarized in Table 1.

TABLE 1. SYSTEM REQUIREMENTS AND DESIGN FACTORS

Satellite Life (minimum)	1 year
Orbit Period	90 min
Dewar Initial Helium Load	300 kg
Maximum Thrust per Nozzle	650 dynes
Thrust Tolerance Open Loop	±2 percent of commanded value
Transient Response Parameters	Damping Factor = 0.707 Natural Frequency = 10 Hz
Sensitivity (minimum thrust increment) Closed Loop	0.1 dynes
Allowable Unbalanced Drag Acceleration	10^{-10} g
Maximum Total Thrust Required	1300 dynes
Helium Dewar Heat Leak Range	0.2326 to 0.1849 W
Nominal Dewar Temperature	1.6°K
Allowable Dewar Temperature Range	1.5 to 1.7°K
Boiloff Delivered Temperature Range	300° to 375°K
Power Penalty (system mass per W)	1.5 kg/W

III. HELIUM THRUSTER PERFORMANCE

The ideal (one-dimensional, frictionless) vacuum specific impulse of a helium nozzle at an area ratio of four was calculated using the ODE computer program [1] for a chamber temperature and pressure of 300°K and 3 torr, respectively. This yielded a characteristic velocity of 3566 ft/sec and a vacuum specific impulse of 168.9 lbf sec/lbm. However, at the low chamber pressures and small throat diameters, the throat Reynolds' number will be quite low (approximately 100) and there will be considerable friction loss. Tests conducted at Stanford University [2] on a 20 deg half angle conical nozzle with a 1.37 mm (0.054 in.) diameter throat, and area ratio and chamber conditions as above, gave vacuum specific impulse figures of approximately 130 lbf sec/lbm. This specific impulse efficiency of approximately 0.77 has been substantiated in as-yet unpublished tests at MSFC with a nozzle of similar geometry but a larger throat diameter of 5.01 mm (0.196 in.). It therefore appears that a specific impulse of 130 lbf sec/lbm, or possibly larger, is attainable for the planned propulsion system. However, for the system developed in this report, a value of 115 lbf sec/lbm was used for the specific impulse to provide some contingency. Even this conservative value is very good in comparison with alternative propellants, particularly when it is available as a waste gas from the dewar boiloff.

IV. PROPULSION SYSTEM DESCRIPTION

The main problem to be overcome on the supply side of the propulsion system is in accommodating (with minimum waste) the inequality between the boiloff produced by an arbitrarily varying heat leak into the dewar and the on-demand varying flow rate required by the thrusters. Conversion of the maximum dewar boiloff due to heat leak (0.2326 W) and the maximum required thrust (1300 dynes at 115 lbf sec/lbm specific impulse) into helium flow rates gives values of 9.75 and 11.53 mg/sec, respectively, and there is no guarantee that the maximum heat leak would occur at the same time as the maximum thruster requirement. Obviously, at other times the thruster demand would be less than the available boiloff and a surplus of propellant would be available.

A system which could save or store the excess flow to be used to cover the periods of deficiency is most desirable, especially if it can be accomplished without a weight or power penalty. Such a system is made possible by exploiting the small, but significant temperature range allowable for the dewar. The large specific heat capacity, low heat of vaporization, low heat leak, and large helium mass relative to the thruster demand flow rate all combine to cause even extremes in the thruster demand and heat leak to result in very small dewar temperature changes over long periods of time. This allows variations in flow rate and heat leak to average out, thus minimizing any dewar venting or heating. Averaging the heat leak extremes gives an average boiloff of 8.75 mg/sec and using Figure 2 gives an orbit average demand of approximately 4.44 mg/sec (500 dynes weighted average thrust at 115 lbf sec/lbm specific impulse). Therefore on a per orbit basis there should be ample propellant boiled off. A schematic of the system capable of accomplishing this is shown in Figure 3. The dewar temperature would be controlled within the allowable range of 1.5° to 1.7°K by activation of a heater on the tank at the low temperature limit and venting non-propulsively at the high temperature limit. The heater would require negligible power due to the very small mass flow rates required and the low latent heat of vaporization of helium. The non-propulsive vent logic would be combined with the attitude control/drag makeup system. When the high temperature limit is approached and venting needed, the controller would select a thruster which was not at full thrust and increase its thrust and that of the opposite one of the back-to-back pair an equal amount. This would effectively vent the extra helium boiloff without the cost

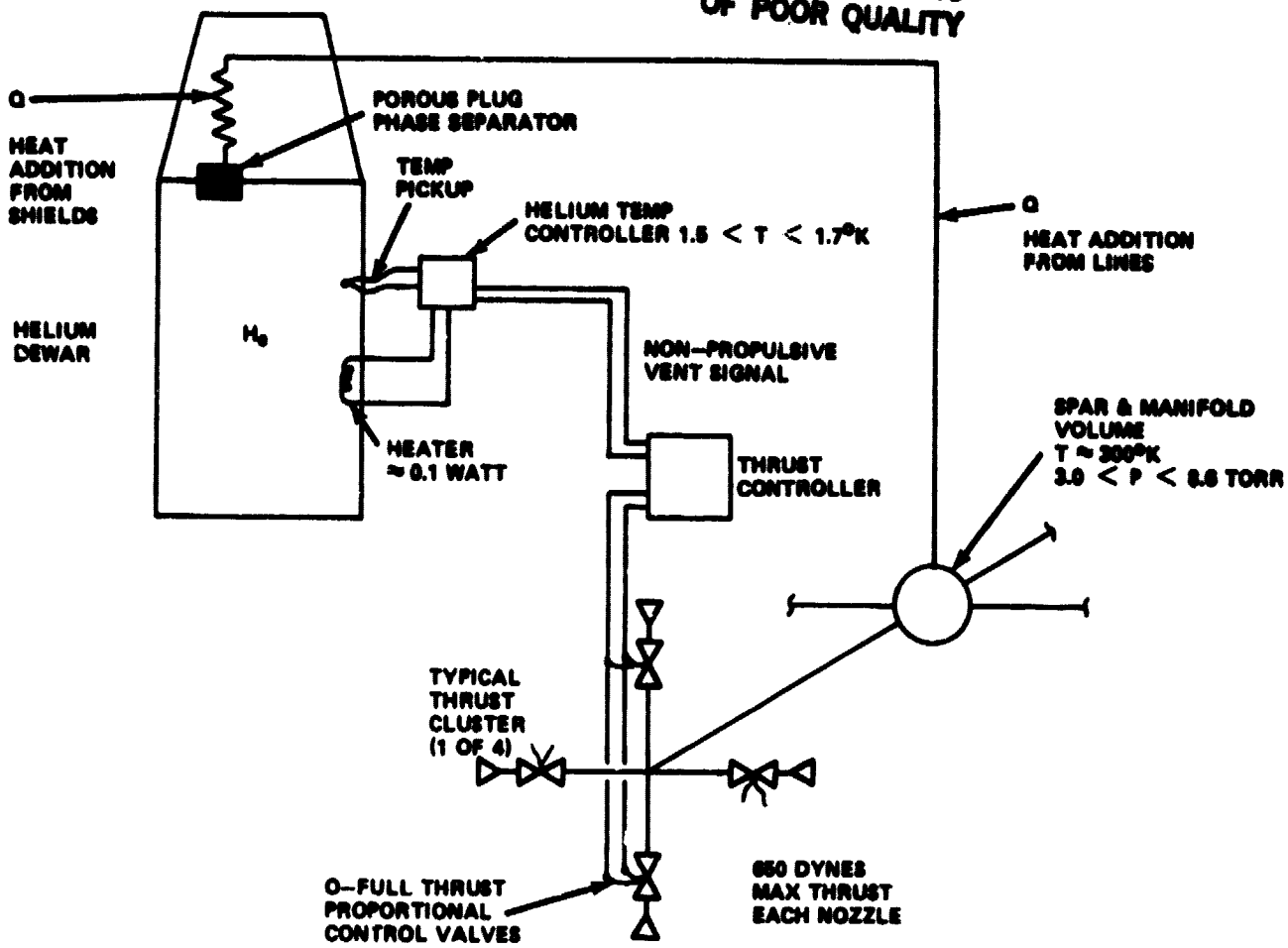

Figure 3. Helium propulsion system schematic.

and complexity of an additional non-propulsive vent valve and lines. Although temperature is indicated as the control variable, pressure could be substituted as the measured variable since it is related to the temperature by the two-phase conditions existing inside the dewar.

A sketch of the distribution system from the dewar to the thrusters is shown in Figure 4. The helium exits the dewar through a porous plug which acts as a phase separator, keeping the liquid helium inside the dewar and allowing the vapor to escape. After the helium leaves the porous plug, it cools the dewar heat shields using the four cooling rings located around the neck tube and exits the dewar into a 1.75 in. OD supply line. This line carries it down the side of the dewar to the support ring (with both sides coupled by the cross braces) which is used as a manifold to distribute the helium to the inside of the four solar array spars. A cluster of four thrusters is fed from the end of each spar. Solar heating of the dewar heat shields, lines and spars raises the helium temperature to at least 300°K by the time it reaches the thrusters. Use of the support ring and solar array spars to deliver the helium saves the weight of additional lines and the large size both reduces pressure loss and provides volume (approximately 117 liters) to reduce pressure transient fluctuations.

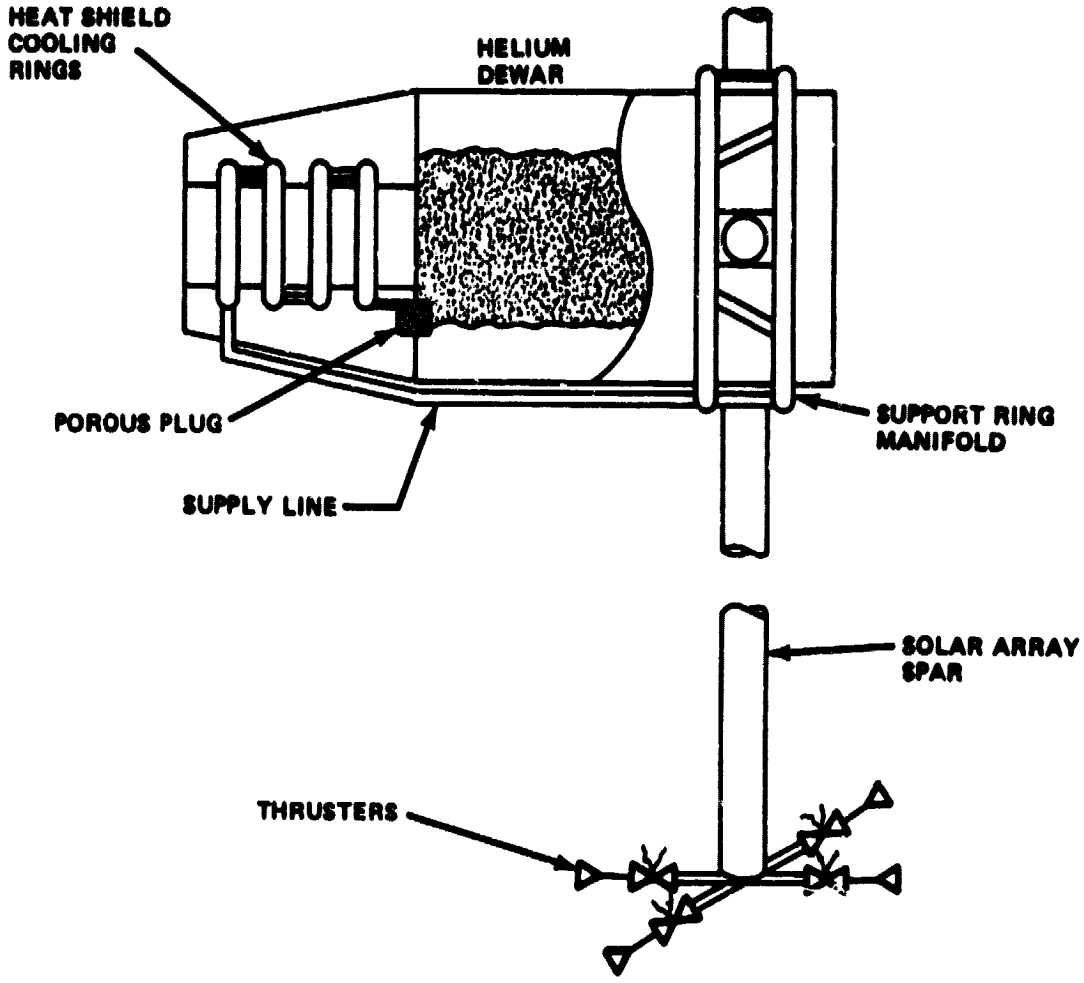

Figure 4. Helium distribution system.

V. SYSTEM ANALYSIS AND SIMULATION

To properly evaluate the flow averaging effect of allowing the dewar temperature to vary to effectively store liquid helium along with energy to convert it to vapor on demand, a relatively rigorous thermodynamic analysis of two-phase helium storage was completed. This analysis included heat addition to the dewar; vapor removed for thruster demand; changes in the temperature, pressure, and density of the stored helium; and transition from one phase to the other. Details of the derivation of the equations and representation of the thermodynamic properties are covered in Appendix A.

A pressure loss equation for the helium gas delivery system is derived in Appendix B and includes use of an average density through each individual flow resistance. A constant temperature is assumed to exist across each resistance element although the temperature can vary from element to element. Checking the Knudsen number, N_{Kn}, inside the 1 in. OD (0.02 in. wall) dewar tube which is the most stringent point in the delivery system; (i.e., where the highest Knudsen numbers would be expected);

$$N_{Kn} = \frac{K\,T}{\sqrt{2}\,P\,\pi\,\delta^2\,r} = 2.85 \times 10^{-3}$$

where

K = Boltzmann constant = 1.38×10^{-16} erg/°K

T = temperature = 213°K

P = pressure = 3.0 torr

δ = molecular diameter (helium) = 2.18×10^{-8} cm

r = tube inside radius = 1.22 cm

verifies the use of the continuum equations since the transition range from continuum to free molecular flow is usually accepted as

$$0.01 < N_{Kn} < 10$$

The resistance factors for use in the delivery system pressure loss calculation are determined in Appendix C. Details on line sizes and lengths can also be found in that section along with flow curves for the porous plug at the dewar exit.

A computer simulation based on the equations and factors developed in the three appendices is presented in Appendix D, along with a sample case. The code was used to evaluate the temperature changes at the extreme (worst case) conditions and the results are shown in Table 2. The first two cases explore the extremes of heat leak and thruster demand for the full dewar with cases three and four the same, but with only 5 percent of the helium remaining. Case five was used as the sample case in Appendix D to get larger, more obvious changes and has a very small amount of helium and an unrealistically low (i.e., 0.0) heat leak coupled with maximum demand. All of these cases show that 150 min of extreme conditions can be tolerated before a temperature limit condition is even approached (starting from a nominal 1.6°K condition). This means that temperature fluctuations during more than one 90 min orbit can be averaged out. Pressure loss through the distribution system at the maximum thruster demand rate of 0.01153 g/sec, and at a low dewar pressure of 4.20 torr (1.533°K saturation temperature) was found to be 0.385 torr which is considered satisfactory.

CONCLUSIONS

A propulsion system utilizing the boiloff helium gas from the experiment package dewar can be made feasible by exploiting the small allowable temperature range of the two-phase helium dewar. This small temperature fluctuation allows liquid helium and sufficient heat to vaporize it to be stored in the dewar for later use when a high thruster demand flowrate is required. The temperature limits of 1.5° to 1.7°K allow a sufficient range to average the expected variations in heat leak and thruster demand over more than one 90 min orbit even under worst case conditions.

TABLE 2. COMPUTER SIMULATION RESULTS FOR EXTREME CONDITIONS

Initial Temperature 1.6°K

Saturation Pressure 5.689 torr

Case	Conditions			Results @ 150 min	
	Initial Helium Mass (grams)	Demand Flow (g/sec)	Heat Leak (W)	Temperature (°K)	Saturation Pressure (torr)
1	300,000	0.01153 (Max)	0.1849 (Min)	1.598	5.650
2	300,000	0.00 (Min)	0.2326 (Max)	1.605	5.800
3	15,000	0.01153 (Max)	0.1849 (Min)	1.588	5.388
4	15,000	0.0 (Min)	0.2326 (Max)	1.634	6.561
5	550	0.01153 (Max)	0.0 (Below Min.)	1.533	4.204

REFERENCES

1. Gordon, S. and McBride, B. J.: Computer Program for Calculation of Complex Equilibrium Compositions, Rocket Performance, Incident and Reflected Shocks, and Chapman-Jouquet Detonations. NASA SP-273, 1971.

2. Bull, John S.: Precise Attitude Control of the Stanford Relativity Satellite. SUDDAR No. 452, Stanford University, Stanford, California, November 1971.

3. Hendricks, J. B.: Characterization of Superfluid Porous Plug Performance. Proceedings of the 9th International Engineering Conference, Butterworth and Co., London, England, 1982, pp. 190-193.

4. Krause, Helmut G.: Orbital Aerodynamics for the Gravity Probe B, Configuration No. 27B, September 18, 1981. MSFC Internal Memo/ED33, December 11, 1981.

APPENDIX A

HELIUM DEWAR THERMODYNAMIC DERIVATION

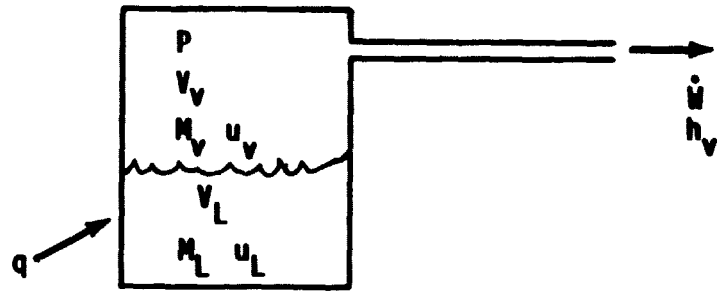

First law energy balance (neglecting potential and kinetic energy):

$$\delta Q - \delta W + (u + P_v)_{in}\, \delta M_{in} - (u + P_v)_{out}\, \delta M_{out} = d U$$

or in time rate of change with δW and δM_{in} equal to 0.

$$q\, dt - h_v \left.\frac{dM}{dt}\right]_{out} dt = d U$$

$$q - h_v \dot{W} = \frac{dU}{dt} \qquad (1)$$

The dewar internal energy, U, is the sum of the vapor and liquid portions

$$U = M_v u_v + M_L u_L$$

Substituting the following equalities

$$M = \rho V$$

$$u = h - Pv$$

$$\rho = 1/v$$

$$V_V = V_D - V_L$$

$$h_v = h_L + h_{fg}$$

and rearranging gives an expression for the internal energy in properties dependant on the saturation, T, and a time dependent variable, the liquid volume, V_L.

$$U = V_L (\rho_V (h_L + h_{fg}) - P) - V_L (\rho_V (h_L + h_{fg}) - \rho_L h_L)$$

Functionally then, U depends only on dewar temperature and time

$$U = f(T,t)$$

in differential form

$$dU = \frac{\partial U}{\partial t}\Big]_T dt + \frac{\partial U}{\partial T}\Big]_t dT$$

and the time derivative of the internal energy is

$$\frac{dU}{dt} = \frac{\partial U}{\partial t}\Big]_T + \frac{\partial U}{\partial T}\Big]_t \frac{dT}{dt} \qquad (2)$$

Evaluating the time partial using the expression for internal energy above gives

$$\frac{\partial U}{\partial t}\Big]_T = -(\rho_v (h_L + h_{fg}) - \rho_L h_L) \frac{\partial V_L}{\partial t}$$

An expression for the liquid volume was found as follows (assuming the mass in the tank exceeds $\rho_V V_D$). The total mass is the sum of the mass of the vapor and liquid

$$M_T = \rho_V V_V + \rho_L V_L = \rho_V (V_D - V_L) + \rho_L V_L$$

and solving for liquid volume

$$V_L = \frac{M_T - \rho_V V_D}{(\rho_L - \rho_V)}$$

If the thruster demand, W, is constant, the existing mass in the dewar at any time is the initial loaded mass less the flow rate times the elapsed time

$$M_T = M_i - W\,t$$

Substitution gives the desired liquid volume relationship

$$V_L = \frac{M_i - Wt - \rho_V V_D}{(\rho_L - \rho_V)}$$

and the time partial derivative of the liquid volume is

$$\frac{\partial V_L}{\partial t} = - \frac{\dot{W}}{(\rho_L - \rho_V)}$$

giving the time partial derivating for internal energy below

$$\left.\frac{\partial U}{\partial t}\right]_T = \left[\frac{\rho_V\, h_{fg}}{(\rho_L - \rho_V)} - h_L\right] \dot{W} \qquad (3)$$

The temperature partial derivative for the internal energy was found similarly

$$\left.\frac{\partial U}{\partial T}\right]_t = (V_D - V_L)\,(h_L + h_{fg})\,\frac{\partial \rho_V}{\partial T} + \left[(\rho_L - \rho_V)\,h_L - \rho_V\, h_{fg}\right]\frac{\partial V_L}{\partial T}$$

$$+ \left[\rho_V\, V_D + (\rho_L - \rho_V)\, V_L\right]\frac{\partial h_L}{\partial T} + \rho_V\,(V_D - V_L)\,\frac{\partial h_{fg}}{\partial T} - V_D\,\frac{\partial P}{\partial T}$$

and, from the expression for liquid volume, the temperature partial derivative for liquid volume is

$$\frac{\partial V_L}{\partial T} = \left[\frac{M_i - \dot{W}t - \rho_V\, V_D}{(\rho_L - \rho_V)^2} - \frac{V_D}{(\rho_L - \rho_V)}\right]\frac{\partial \rho_V}{\partial T}$$

After substitution and simplifying, the temperature partial derivative for internal energy is given below

$$\left.\frac{\partial U}{\partial T}\right]_t = \left[h_{fg}\frac{\partial \rho_V}{\partial T}\left[1+\left(\frac{\rho_V}{\rho_L-\rho_V}\right)^2\right]+\rho_V\frac{\partial h_{fg}}{\partial T}\left[1+\frac{\rho_V}{(\rho_L-\rho_V)}\right]-\frac{\partial P}{\partial T}\,\mathrm{Conv}_1\right] V_D$$

$$+\left[\frac{\partial h_L}{\partial T}-\frac{\rho_V}{(\rho_L-\rho_V)}\frac{\partial h_{fg}}{\partial T}-\frac{h_{fg}}{(\rho_L-\rho_V)}\frac{\partial \rho_V}{\partial T}\left[1+\frac{\rho_V}{(\rho_L-\rho_V)}\right]\right](M_i-\dot{W}t) \qquad (4)$$

Rearranging equation (2) to get the dewar saturation temperature time derivative

$$\frac{dT}{dt}=\frac{\left.\frac{dU}{dt}-\frac{\partial U}{\partial t}\right]_T}{\left.\frac{\partial U}{\partial T}\right]_t}=\frac{[q-(h_L+h_{fg})\dot{W}]-\left[\frac{\rho_V}{(\rho_L-\rho_V)}h_{fg}-h_L\right]\dot{W}}{\left.\frac{\partial U}{\partial T}\right]_t}$$

abbreviating equation (4) into

$$\left.\frac{\partial U}{\partial T}\right]_t = [f_1(T)]_1\,V_D+[f_2(T)]_2\,(M_i-\dot{W}t)$$

and substituting, gives an expression to be solved for the dewar saturation temperature as a function of time with given initial condition and constant thruster demand, $\dot{W}$.

$$\frac{dT}{dt}=\frac{q-h_{fg}\dot{W}\left[1+\frac{\rho_V}{(\rho_L-\rho_V)}\right]}{[f_1(T)]_1\,V_D+[f_2(T)]_2\,(M_i-\dot{W}t)} \qquad (5)$$

Since the variables could not be separated, a numerical integration was required. The properties were defined by curve fits over the range of 1.4 to 1.8°K. Methods and constants follow:

q = Const = input – heat leak, J/sec (W)

$\dot{W}$ = Const = input -- demand flow rate, g/sec

T_i = Const = Input – initial dewar temperature, °K

M_i = Const = input – initial helium mass, g

V_D = Const = input – dewar volume, L

ρ_L = Const = 145.1 g/L – helium liquid density, g/L

Helium vapor is assumed to obey the perfect gas law

$$\rho_V = \frac{P}{RT} \quad g/L \qquad (P, \text{torr}; T°K) \qquad (6)$$

$$R = 15.5938 \quad \frac{\text{torr L}}{g\,°K}$$

$$\frac{\partial \rho_V}{\partial T} = \left[-\frac{P}{RT^2} + \frac{1}{RT}\frac{\partial P}{\partial T} \right] \quad \frac{g}{L\,°K} \qquad (P, \text{torr}; T, °K; \frac{\partial P}{\partial T}, \frac{\text{torr}}{°K}) \qquad (7)$$

$$P = e^{(C_o + C_1(1/T) + C_2 T^2)} \quad \text{torr } (T,°K) \qquad (8)$$

C_o = 7.5959

C_1 = -9.9416 °K

C_2 = 0.13913 $°K^{-2}$

$$\frac{\partial P}{\partial T} = [-C_1(1/T^2) + 2C_2T]\, e^{(C_o + C_1(1/T) + C_2 T^2)} \quad \text{torr}/°K \qquad (T,°K) \qquad (9)$$

Using the Clausius Clapeyron relationship to get h_{fg}

$$\frac{d \ln P}{dT} = \frac{h_{fg}}{RT^2} = -\frac{C_1}{T^2} + 2C_2T$$

$$h_{fg} = (-C_1 R + 2C_2 RT^3)\, Conv_1 \quad J/g \qquad (T,°K) \qquad (10)$$

$$\frac{\partial h_{fg}}{\partial T} = (6C_2 RT^2)\, Conv_1 \quad J/g°K \qquad (T,°K) \qquad (11)$$

$$h_L = h_{L_{base}} + \int_{T_B}^{T} dh_L$$

$$dh_L = C_p\, dT - \left[T\left(\frac{\partial v_L}{\partial T}\right)_p - v_L \right] Conv_1\, dP$$

Since $\rho_L \cong$ Const, $\partial v_L/\partial T \cong 0$

and $\int_{P_B}^{P@T} v_L\, dP$ is negligible

$$h_L = h_{L_{base}} + \int_{T_B}^{T} C_p\, dT$$

with

$$C_p = c_o + c_1\, T + c_2\, T^2$$

Let $h_{L_{base}} = 0.$ @ $T_{base} = 1.6°K$, then

$$h_L = c_o T + \frac{c_1}{2} T^2 + \frac{c_2}{3} T^3 + D \quad J/g \quad (T,°K) \tag{12}$$

$c_o = 8.1071\ J/g°K$

$c_1 = -13.2199\ J/g\ °K^2$

$c_2 = 5.7071\ J/g\ °K^3$

$D = -3.842\ J/g$

$$\frac{\partial h_L}{\partial T} = c_o + c_1\, T + c_2\, T^2 \qquad J/g\ °K \qquad (T,°K) \tag{13}$$

$$Conv_1 = 0.13331 \frac{J/L}{torr} \quad .$$

APPENDIX B

HELIUM DELIVERY PRESSURE LOSS DERIVATION

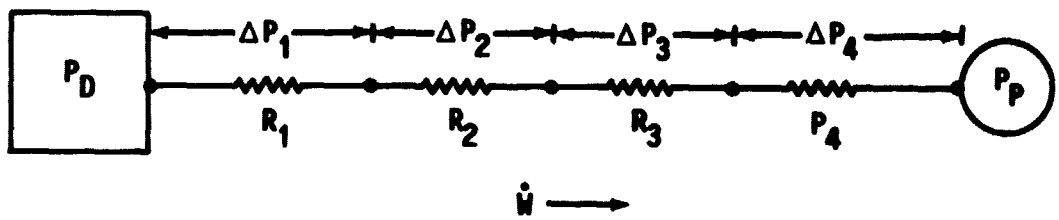

The pressure losses are a combination of frictional losses and expansion/contraction type losses and the loss for each section can be expressed as the sum of these two,

$$\Delta P = f\frac{L}{D}\frac{\dot{W}^2}{A^2\,\bar{\rho}\,2g_c} + K\frac{\dot{W}^2}{A^2\,\bar{\rho}\,2g_c}$$

Since the flow is laminar, the friction factor, f, may be expressed as

$$f = \frac{64.}{N_{Re}} = \frac{64}{\dot{W}\,D/A\,\mu}$$

and the average density, $\bar{\rho}$, can be related to a nominal density, ρ_o, at a nominal pressure, P_o, and the average pressure, $\bar{P}$, by assuming it obeys the perfect gas law $P = \rho RT$, and the temperature is constant across the resistance element.

$$\bar{\rho} = \rho_o\frac{\bar{P}}{P_o}$$

Combining and rearranging

$$\bar{P}\,\Delta P = \frac{64\,\mu\,L\,P_o}{A\,2g_c\,D^2\,\rho_o}\dot{W} + \frac{K\,P_o}{A^2\,2g_c\,\rho_o}\dot{W}^2$$

Applying this equation to a line represented by four sections as an example

$$\bar{P}_1 \Delta P_1 = K_{11} \dot{W} + K_{21} \dot{W}^2$$

$$\bar{P}_2 \Delta P_2 = K_{12} \dot{W} + K_{22} \dot{W}^2$$

$$\bar{P}_3 \Delta P_3 = K_{13} \dot{W} + K_{23} \dot{W}^2$$

$$\bar{P}_4 \Delta P_4 = K_{14} \dot{W} + K_{24} \dot{W}^2$$

Summing

$$(\bar{P}_1 \Delta P_1 + \bar{P}_2 \Delta P_2 + \bar{P}_3 \Delta P_3 + \bar{P}_4 \Delta P_4) = (K_{11} + K_{12} + K_{13} + K_{14}) \dot{W} + (K_{21} + K_{22} + K_{23} + K_{24}) \dot{W}^2 = K_{1T} \dot{W} + K_{2T} \dot{W}^2$$

The average pressure at each section is the upstream pressure at that section less half the pressure loss for that section

$$\bar{P}_1 = (P_D - \Delta P_1/2)$$

$$\bar{P}_2 = (P_D - \Delta P_1 - \Delta P_2/2)$$

$$\bar{P}_3 = (P_D - \Delta P_1 - \Delta P_2 - \Delta P_3/2)$$

$$\bar{P}_4 = (P_D - \Delta P_1 - \Delta P_2 - \Delta P_3 - \Delta P_4/2)$$

and substitution into the above equation gives

$$\dot{K}_{1T} \dot{W} + K_{2T} \dot{W}^2 = \left(P_D \Delta P_1 - \frac{\Delta P_1^2}{2}\right) + \left(P_D \Delta P_2 - \Delta P_1 \Delta P_2 - \frac{\Delta P_2^2}{2}\right) + \left(P_D \Delta P_3 - \Delta P_1 \Delta P_3 - \Delta P_2 \Delta P_3 - \frac{\Delta P_3^2}{2}\right) + \left(P_D \Delta P_4 - \Delta P_1 \Delta P_4 - \Delta P_3 \Delta P_4 - \frac{\Delta P_4^2}{2}\right)$$

Rearranging and factoring

$$K_{1T}\,\dot{W} + K_{2T}\,\dot{W}^2 = P_D\,(\Delta P_1 + \Delta P_2 + \Delta P_3 + \Delta P_4) - \frac{1}{2}\,(\Delta P_1 + \Delta P_2 + \Delta P_3 + \Delta P_4)\,(\Delta P_1 + \Delta P_2 + \Delta P_3 + \Delta P_4)$$

Recognizing that the bracketed terms are the overall loss, ΔP_T, the expression simplifies to

$$K_{1T}\,\dot{W} + K_{2T}\,\dot{W}^2 = P_D\,\Delta P_T - \frac{1}{2}\,\Delta P_T^2$$

Solving the quadratic in $\dot{W}$ gives

$$\dot{W} = \frac{-K_{1T} + \sqrt{K_{1T}^2 - 4\,K_{2T}\,(\frac{1}{2}\,\Delta P_T^2 - P_D\,\Delta P_T)}}{2\,K_{2T}}$$

or alternately for ΔP_T

$$\Delta P_T = P_D - \sqrt{P_D^2 - 2\,(K_{1T}\,\dot{W} + K_{2T}\,\dot{W}^2)}$$

APPENDIX C

HELIUM DELIVERY PRESSURE LOSS RESISTANCE FACTORS DETERMINATION

Resistance Factors for Porous Plug

Flow characteristics (Fig. 5) for the porous plug were obtained from Reference 3. The sharp change of slope of these curves was referred to as the "critical mass flow rate" point and because of it the curve required two resistance representations. The unit area of the tested plug, A_p, was the same as that to be used on the GPB dewar. Temperature range for these equations is $1.6 < T < 1.8$ °K.

The dividing line for "critical" flow was estimated to be

$$\dot{W}_{crit} = [1.5 + 10\,(T - 1.65)] \times 10^{-3} \quad \text{g/sec} \qquad (T, °K)$$

The pressure-flow relationship for flow below critical, i.e., low resistance, was

$$\Delta P = 0.5769\,\dot{W} \quad \text{torr} \qquad (\dot{W}, \text{g/sec})$$

$$\bar{P}\,\Delta P = 0.5769\,\bar{P}\,\dot{W} \quad .$$

If $\bar{P} \approx P_D$

$$\bar{P}\,\Delta P = 0.5769\,P_D\,\dot{W} \quad \text{torr}^2 \qquad (\dot{W}, \text{g/sec};\ P_D, \text{torr})$$

with

$$K_{11} = 0.5769\,P_D \quad .$$

Above critical flow, i.e., high resistance,

$$\dot{W} = \left[1.65 + \frac{1.90}{0.2}\,[T - 1.65] + \frac{3.65}{4.50 \times 10^{-3}}\,\Delta P\right] \times 10^{-3} \quad \text{g/sec} \qquad (T, °K;\ \Delta P, \text{torr})$$

$$\Delta P = 1.233\,\dot{W} - 1.233\,[1.65 \times 10^{-3}\,(1 + 9.5\,(T/1.65 - 1))]$$

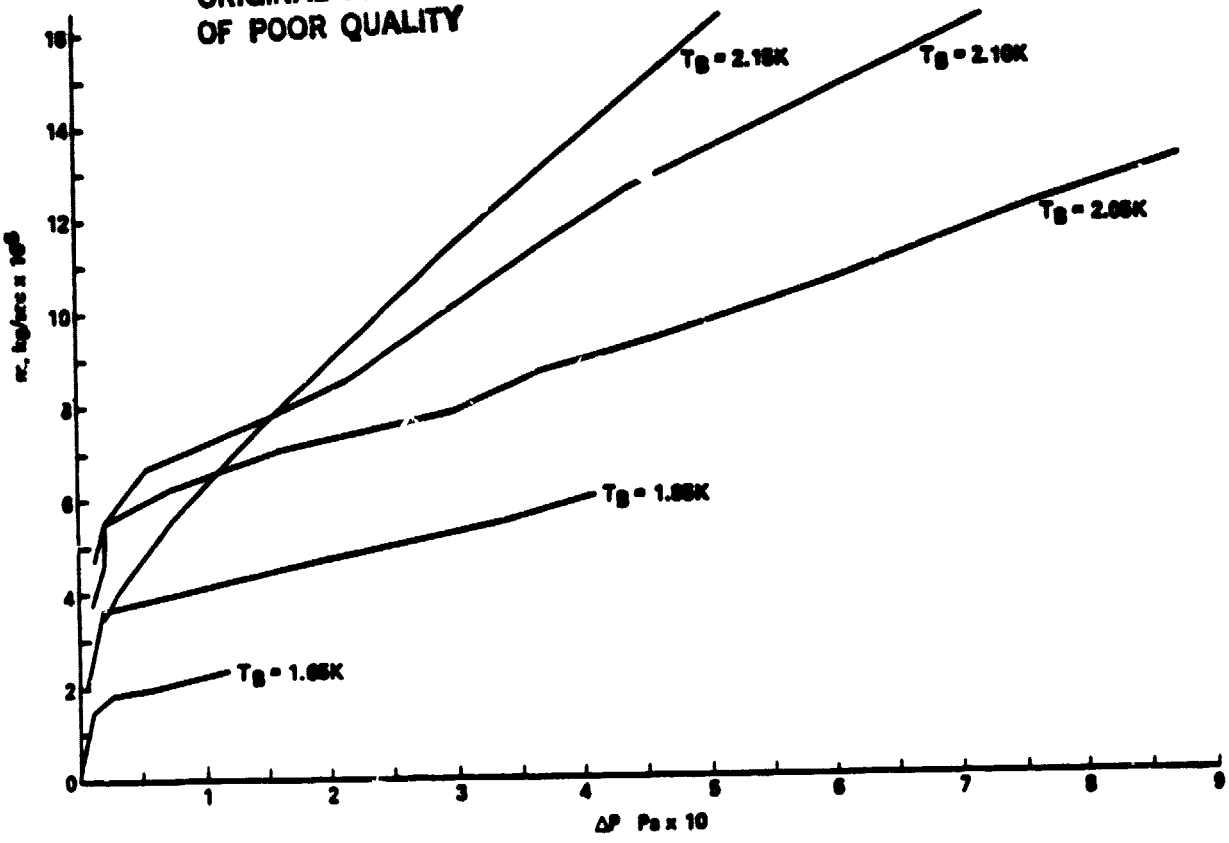

Figure 5. Porous plug flow versus pressure drop.

$$\bar{P}\,\Delta P = 1.233\,\bar{P}\,\dot{W} - 1.233\,\bar{P}\,[1.65 \times 10^{-3}\,(1 + 9.5\,(T/1.65 - 1))]$$

If $\bar{P} \approx P_D$

$$P\,\Delta P = 1.233\,P_D\,\dot{W} - 1.233\,P_D\,[1.65 \times 10^{-3}\,(1 + 9.5\,(T/1.65 - 1))] \qquad \text{torr}^2$$

$$= K_{11}\,\dot{W} + C \qquad (P_D, \text{torr};\ T, {}^\circ K)$$

where

$$K_{11} = 1.233\,P_D$$

$$C = -1.233\,P_D\,[1.65 \times 10^{-3}\,(1 + 9.5\,(T/1.65 - 1))] \quad .$$

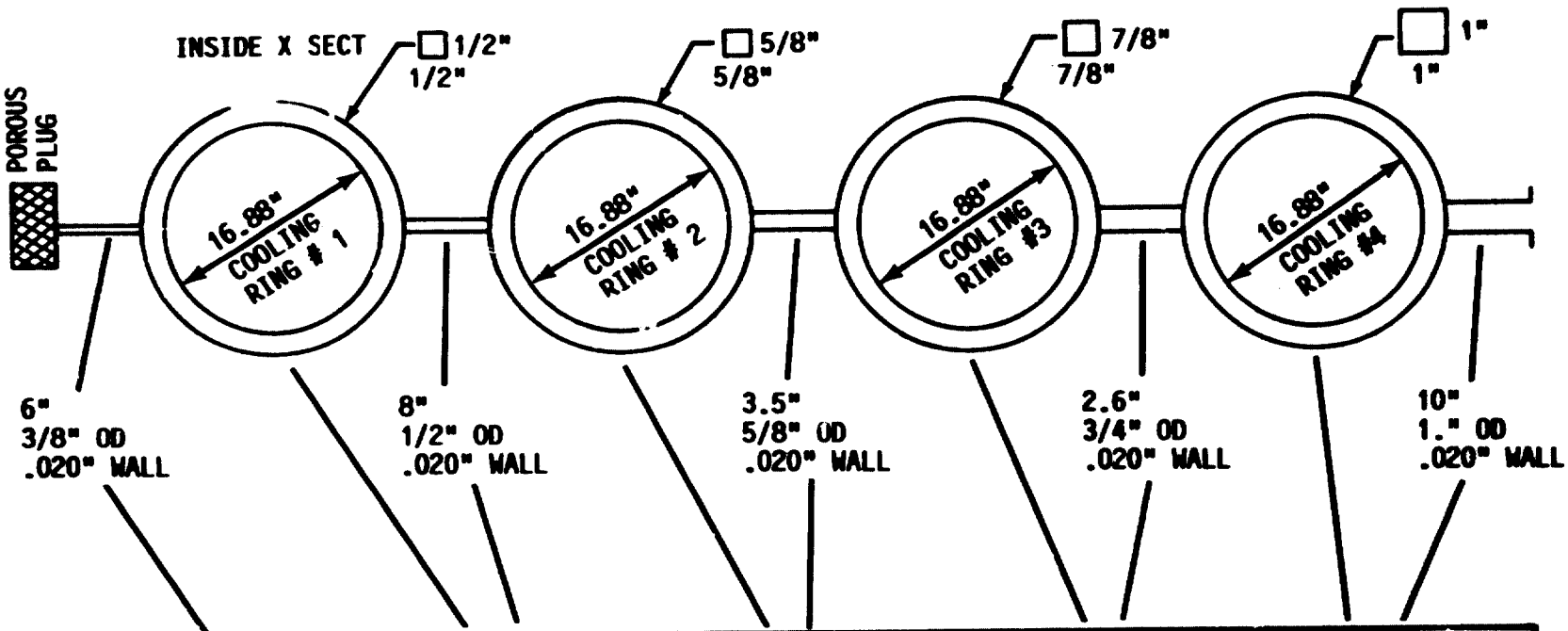

T °K	5.	30.	96.	163.	213.
$\mu \frac{LB}{FT - SEC}$ @ 1 PSIA	$.846 \times 10^{-6}$	3.09×10^{-6}	6.14×10^{-6}	8.87×10^{-6}	10.60×10^{-6}
$\rho_o \frac{LB}{FT^3}$	.04190	.006917	.002305	.001276	.0009768
P_o TORR	51.706	51.706	51.706	51.706	51.706

Figure 6. Cooling rings schematic.

The extra term C is not common to the other resistance elements since they do not have the transition point in the $\dot{W}$, ΔP curve.

Equation for Helium Delivery System Pressure Loss Simulation for Computer Program

$\dot{W} \sim$ g/sec

ΔP and $P_D \sim$ torr

$$\Delta P = P_D - \sqrt{P_D^2 - 2 (K_{1T} \dot{W} + K_{2T} \dot{W}^2 + C)}$$

$\dot{W}$ above $\dot{W}_{crit}$

$$C = - 1.233 P_D [1.65 \times 10^{-3} (1 + 9.5 (T_D/1.65 - 1))]$$

$$K_{1T} = 121.97 + 1.233 P_D$$

$$K_{2T} = 605.6$$

$\dot{W}$ below $\dot{W}_{crit}$

$$C = 0.0$$

$$K_{1T} = 121.97 + 0.577 P_D$$

$$K_{2T} = 605.6$$

where

$$\dot{W}_{crit} = (1.5 + 10 (T - 1.65)) \times 10^{-3} \quad \text{g/sec} .$$

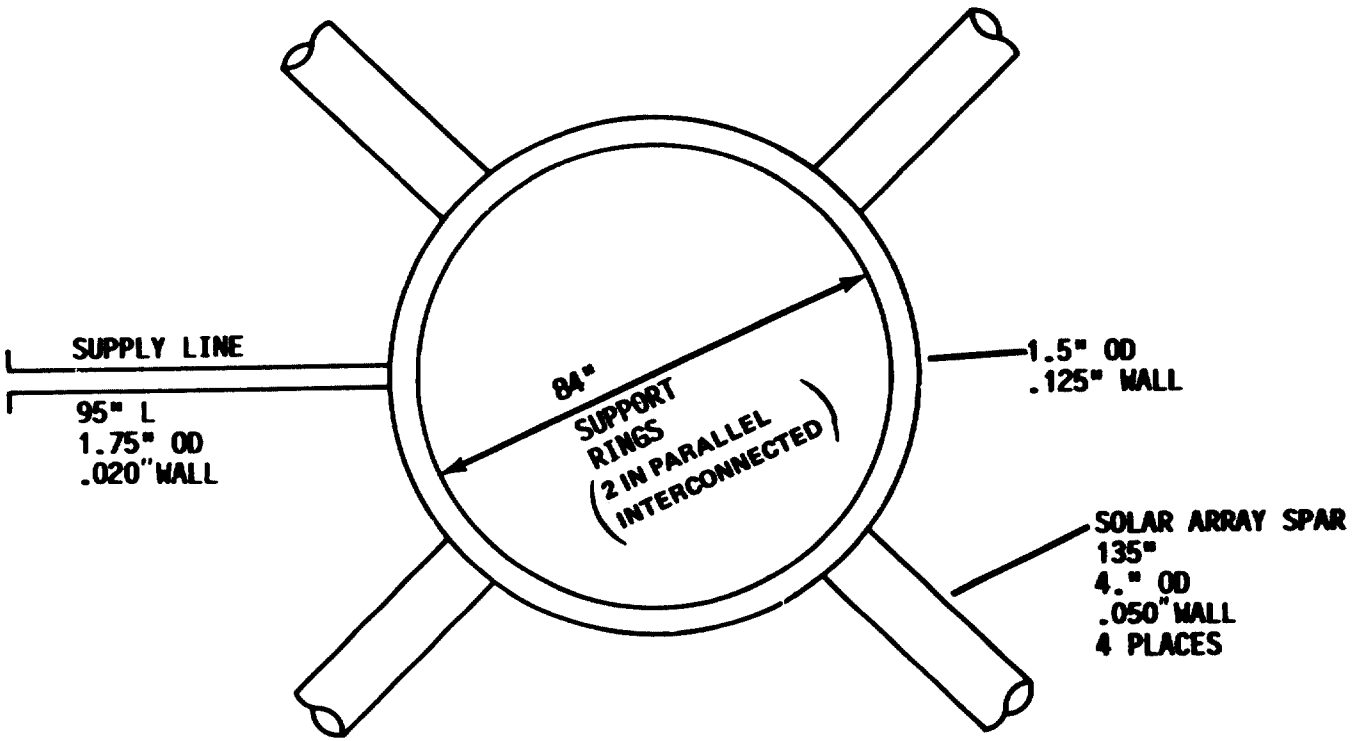

$\mu \frac{LB}{FT - SEC}$ @ 1 PSIA	13.4×10^{-6}
$\rho_o \frac{LB_3}{FT}$	.0006962
P_o TORR	51.706
T °K	300

FOR ALL

Figure 7. Distribution lines schematic.

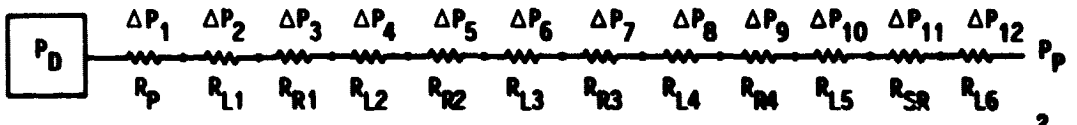

	ELEMENT NO.	ELEMENT	L IN	D_h IN	A_x IN^2	K_c CONTRACTION	K_E EXPANSION	K_1 $TORR^2$-SEC/g * $\dot{w}$	K_2 $TORR^2$-SEC^2/g^2 * $\dot{w}^2$	C $TORR^2$
R_P	1	POROUS PLUG BELOW CRIT.	-	-	-	-	-	$0.5769P_D$	-	0.
		POROUS PLUG ABOVE CRIT.	-	-	-	-	-	$1.233\ P_D$	-	SEE PAGE 23
R_{L1}	2	POROUS PLUG CONNECTOR	6	.335	.0881	-	.68	0.862	60.8	
R_{R1}	3	COOLING RING #1	27.3	.500	2* .2500	-	-	6.861	-	
R_{L2}	4	RING CONNECTOR	8	.460	.1662	.29	.63	7.146	139.9	
R_{R2}	5	COOLING RING #2	27.5	.625	2* .3906	-	-	16.881	-	
R_{L3}	6	RING CONNECTOR	3.5	.585	.2688	.40	.66	7.127	185.0	
R_{R3}	7	COOLING RING #3	27.9	.875	2* .7656	-	-	11.633	-	
R_{L4}	8	RING CONNECTOR	2.6	.710	.3959	.55	.65	6.368	174.4	
R_{R4}	9	COOLING RING #4	28.1	1.000	2* 1.000	-	-	10.722	-	
R_{L5}	10	SUPPLY LINE	10	.96	.724	.28	.47	11.437	42.6	
			95	1.71	2.297	-	.29	19.143	2.3	
R_{SR}	11	SUPPORT RING	132	1.25	2*2* 1.227	-	.33	23.29	.6	
R_{L6}	12	SPAR	135	3.9	$\dot{w}/2$ 11.95	-	-	.503	-	
		Σ	BELOW CRITICAL FLOW					$121.97 + 0.5769R_D$	605.6	0
			ABOVE CRITICAL FLOW					$121.97 + 1.233P_D$	605.6	SEE PAGE 23

APPENDIX D

COMPUTER SIMULATION

The results of the derivations and constants from Appendices A, B, and C were coded into the computer program shown in this section.

Input

NT	Total number of time increments	–
NP	Number of time increments between printouts	–
DTM	Time increment for integration step	Sec
WI	Initial helium mass in dewar (liquid + vapor)	gram
WDT	Demand flow leaving dewar	gram/sec
Q	Heat leak into dewar	watts
VD	Dewar volume	liters
TK	Upper temperature limit of helium in dewar	°K
TL	Lower temperature limit of helium in dewar	°K
TI	Initial temperature of helium in dewar	°K

Output

Line 1 Input

DTM	WI	WCT	Q	VD	TH	TL	TI
Time Increment sec	Initial Mass gram	Demand Flow G/sec	Heat Leak Watts	Dewar Vol Liters	Hi Temp Limit °K	Lo Temp Limit °K	Initial Temp °K

Line 2 Initial Property Values

PD	RG	PP	PRV	DH	PDH	H	PHL
Sat. Press. P torr	Sat. Vap. Density ρ_V G/L	$\partial P/\partial T$ torr/°K	$\partial \rho_V/\partial T$ G/L °K	Latent Heat h_{fg} J/G	$\partial h_{fg}/\partial T$ J/G °K	Liq. Enthalpy h_L J/G	$\partial h_L/\partial T$ J/G °K

Line 3 Initial Pressure Loss

DELP
Delivery system pressure loss at initial conditions torr

Line 4 Initial Thruster Pressure

PV
Pressure delivered to thruster at initial conditions torr

Line 5 Current Property Values

As line 2 without PD
Property values at (current time - 1 time increment)

Line 6 Current Dewar Conditions

TM	PD	T	DTDTM	W
Elapsed Time t sec	Sat. Press. P torr	Dewar Temp. T °K	Temp. Rate of Change dT/dt °K/sec	Helium Mass (Liq + Vap) gram

Successive Line Pairs

Lines 5 & 6 Repeated

Next to Last

Same as Line 3 for Final Conditions

Last

Same as Line 4 for Final Conditions

```
C   DEFINE PROPERTY FUNCTIONS
      P(T)  = EXP(C0 + C1/T + C2*T**2)
      RV(T) = P(T)/(R*T)
      PPPT(T) = (2.*C2*T -.C1/T**2)*P(T)
      PRVPT(T) = (-P(T)/T + PPPT(T))/(R*T)
      DHFG(T) = (2.*C2*R*T**3 - C1*R)*CV1
      PDHPT(T) = CV1*6.*C2*R*T**2
      HL(T) = D + SC0*T + (SC1/2.)*T**2 + (SC2/3.)*T**3
      PHLPT(T) = SC0 + SC1*T + SC2*T**2
C
      READ(7,12) NT
      READ(7,12) NP
      READ(7,11) DTM
      READ(7,11) WI
      READ(7,11) WDT
      READ(7,11) Q
      READ(7,11) VD
      READ(7,11) TH
      READ(7,11) TL
      READ(7,11) TI
      WRITE(2,10) DTM,WI,WDT,Q,VD,TH,TL,TI
C   SET UP CONSTANTS
      CV1 =.0.13331
      R   = 15.594
      C0  =.7.5959
      C1  = -9.9416
      C2  =.0.13913
      SC0 = 8.1071
      SC1 = -13.2199
      SC2 = 5.7071
      D   = -3.842
C
      N=NT/NP
C
      RL  = 145.1
C . INITIALIZE
      TM = 0.0
      T  = TI
C   PRINT INITIAL PROPERTY VALUES
      PD = P(T)
      RG = RV(T)
      PP = PPPT(T)
      PRV = PRVPT(T)
      DH = DHFG(T)
      PDH = PDHPT(T)
      H  = HL(T)
      PHL = PHLPT(T)
      WRITE(2,10) PD,RG,PP,PRV,DH,PDH,H,PHL
C   CALC. PRESS. LOSS TO THRUSTER PLENUM
      PD = P(T)
      CALL PLOSS(WDT,PD,T)
```

```
C   INTEGRATE TEMP. RATE OF CHANGE FUNCTION
      DO 2 I=1,N
      DO 1 J=1,NP
      DH = DHFG(T)
      PRV =.PRVPT(T)
      PDH = PDHPT(T)
      RG = RV(T)
      PHL = PHLPT(T)
      RR = RG/(RL - RG)
      W =WI - WDT*TM
      IF(RG*VD.GE.W) GO TO 4
      B1 = VD*(DH*PRV*(1. + RR**2) + RG*PDH*(1. + RR) - CV1*PPPT(T))
      B2 = PHL - RR*PDH - DH*PRV*(1. + RR)/(RL - RG)
      DTDTM = (Q - DH*(1. + RR)*WDT)/(B1 + B2*W)
      T = T + DTDTM*DTM
      PD = P(T)
      TM = TM + DTM
      IF (T  -TH) 3,3,4
    3 IF.(TL - T) 1,1,4
    1 CONTINUE
      WRITE(2,10) RG,PP,PRV,DH,PDH,H,PHL
    2 WRITE(2,10) TM,PD,T,DTDTM,W
    4 CALL PLOSS(WDT,PD,T)
   10 FORMAT(1X,9(1X,E12.5))
   11 FORMAT(F10.5)
   12 FORMAT(I6)
      STOP
      END
C
C
      SUBROUTINE PLOSS(WDT,PD,T)
      WDBO = WDT
      WDCRT= (1.5.+ 10.*(T - 1.65))*1.0E-3
      CK2T = 605.6
      IF(WDBO -. WDCRT) 1,2,2
C   FLOW RATE BELOW CRITICAL
 1    C = 0.0
      CK1T = 121.97 + (5.77E-1)*PD
      GO TO 3
C   FLOW RATE ABOVE CRITICAL
 2    C = -1.233*PD*(1.65E-3*(1. + 9.5*(T/1.65 -.1.)))
     .CK1T.= 121.97 + 1.233*PD
 3   ..DELP = PD - SQRT(PD**2 - 2.*(CK1T*WDBO + CK2T*WDBO**2 + C))
      PV = PD - DELP
      WRITE(2,4) DELP,PV
 4    FORMAT(1X,E12.5)
     .RETURN
      END
```

```
B>TYPE FORT07.DAT
   900
    20
10.
550.
.01153
0.0
2218.
1.8
1.4
1.6


B>OPB
```

SAMPLE OUTPUT
(CASE 5 FROM TABLE 2)

```
 .10000E+02   .55000E+03   .11530E-01   -.00000E+01   .22180E+04   .18000E+01   .14000E+01   .16000E+01
 .56892E+01   .22802E+00.  .24627E+02    .84451E+00.  .23036E+02   .44425E+01  -.18835E-04   .15654E+01
.28105E+00
.54082E+01
 .22692E+00.  -.24627E+02   .84169E+00    .23031E+02   .44353E+01. -.18835E-04    .15589E+01
-.20000E+03    .56556E+01.  .15986E+01   -.68622E-05   .54781E+03
 .22577E+00   .24627E+02    .83870E+00   -.23024E+02   .44277E+01   -.18835E-04   .15520E+01
 .40000E+03   -.56219E+01    .15973E+01   -.68875E-05   .54550E+03
-.22461E+00   -.24627E+02    .83572E+00   -.23018E+02  -.44201E+01   -.18835E-04    .15451E+01
 .60000E+03    .55883E+01   .15959E+01   -.69131E-05   .54320E+03
-.22346E+00   -.24627E+02    .83273E+00    .23012E+02   .44124E+01  -.18835E-04    .15382E+01
 .80000E+03   .55547E+01    .15945E+01   -.69388E-05   .54089E+03
 .22230E+00    .24627E+02    .82973E+00   .23006E+02   .44047E+01   -.18835E-04   .15313E+01
 .10000E+04    .55212E+01   .15931E+01   -.69648E-05   .53859E+03
 .22115E+00.   .24627E+02    .82673E+00   -.23000E+02  -.43970E+01  -.18835E-04   .15243E+01
 .12000E+04   -.54877E+01    .15917E+01   -.69910E-05   .53628E+03
-.21999E+00   -.24627E+02    .82372E+00   -.22994E+02   .43892E+01  -.18835E-04   -.15174E+01
 .14000E+04    .54542E+01    .15903E+01   -.70175E-05   .53397E+03
 .21883E+00   -.24627E+02    .82071E+00    .22988E+02   .43815E+01   -.18835E-04   -.15105E+01
 .16000E+04   -.54207E+01    .15889E+01   -.70442E-05   .53167E+03
 .21768E+00   -.24627E+02    .81769E+00   -.22981E+02   .43737E+01   -.18835E-04   -.15036E+01
 .18000E+04    .53872E+01   .15876E+01   -.70711E-05   .52936E+03
 .21652E+00   -.24627E+02    .81467E+00   -.22975E+02   .43659E+01  -.18835E-04   .14966E+01
 .20000E+04    .53538E+01   -.15861E+01   -.70983E-05   .52705E+03
 .21537E+00    .24627E+02   -.81164E+00   -.22969E+02   .43581E+01  -.18835E-04    .14897E+01
 .22000E+04    .53205E+01    .15846E+01   -.71257E-05   .52475E+03
 .21421E+00    .24627E+02    .80860E+00    .22963E+02   .43502E+01   -.18835E-04   .14828E+01
 .24000E+04    .52871E+01   -.15832E+01   -.71534E-05   .52244E+03
 .21305E+00.   .24627E+02    .80556E+00    .22957E+02   .43424E+01  -.18835E-04    .14758E+01
 .26000E+04    .52538E+01    .15818E+01   -.71813E-05   .52014E+03
 .21190E+00   -.24627E+02    .80251E+00    .22950E+02   .43345E+01   -.18835E-04   -.14689E+01
 .28000E+04    .52205E+01    .15803E+01   -.72095E-05   .51783E+03
 .21074E+00    .24627E+02    .79946E+00   -.22944E+02   .43265E+01   -.18835E-04   -.14619E+01
 .30000E+04    .51872E+01   -.15789E+01   -.72380E-05   .51553E+03
 .20958E+00    .24627E+02    .79640E+00   -.22938E+02   .43186E+01   -.18835E-04    .14550E+01
 .32000E+04    .51540E+01    .15774E+01   -.72667E-05   .51322E+03
 .20842E+00    .24627E+02    .79333E+00    .22932E+02   .43106E+01  -.18835E-04   -.14480E+01
 .34000E+04    .51208E+01    .15760E+01   -.72957E-05   .51091E+03
 .20727E+00    .24627E+02    .79026E+00   -.22925E+02   .43026E+01   -.18835E-04   -.14410E+01
 .36000E+04    .50876E+01   -.15745E+01   -.73250E-05   .50861E+03
```

```
 .20611E+00   .24627E+02   .78718E+00   .22919E+02   .42946E+01  -.18835E-04   .14341E+01
 .38000E+04   .50545E+01   .15731E+01  -.73544E-05   .50630E+03
 .20495E+00   .24627E+02   .78410E+00   .22913E+02   .42866E+01  -.18835E-04   .14271E+01
 .40000E+04   .50214E+01   .15716E+01  -.73845E-05   .50400E+03
 .20379E+00   .24627E+02   .78101E+00   .22906E+02   .42785E+01  -.18835E-04   .14201E+01
 .42000E+04   .49883E+01   .15701E+01  -.74146E-05   .50169E+03
 .20263E+00   .24627E+02   .77792E+00   .22900E+02   .42704E+01  -.18835E-04   .14132E+01
 .44000E+04   .49552E+01   .15686E+01  -.74451E-05   .49938E+03
 .20148E+00   .24627E+02   .77481E+00   .22894E+02   .42623E+01  -.18835E-04   .14062E+01
 .46000E+04   .49222E+01   .15671E+01  -.74758E-05   .49708E+03
 .20032E+00   .24627E+02   .77170E+00   .22887E+02   .42541E+01  -.18835E-04   .13992E+01
 .48000E+04   .48892E+01   .15656E+01  -.75069E-05   .49477E+03
 .19916E+00   .24627E+02   .76859E+00   .22881E+02   .42460E+01  -.18835E-04   .13922E+01
 .50000E+04   .48563E+01   .15641E+01  -.75382E-05   .49247E+03
 .19800E+00   .24627E+02   .76547E+00   .22874E+02   .42378E+01  -.18835E-04   .13852E+01
 .52000E+04   .48233E+01   .15626E+01  -.75699E-05   .49016E+03
 .19684E+00   .24627E+02   .76234E+00   .22868E+02   .42296E+01  -.18835E-04   .13782E+01
 .54000E+04   .47905E+01   .15611E+01  -.76019E-05   .48785E+03
 .19568E+00   .24627E+02   .75921E+00   .22862E+02   .42213E+01  -.18835E-04   .13713E+01
 .56000E+04   .47576E+01   .15596E+01  -.76342E-05   .48555E+03
 .19452E+00   .24627E+02   .75607E+00   .22855E+02   .42130E+01  -.18835E-04   .13643E+01
 .58000E+04   .47248E+01   .15580E+01  -.76669E-05   .48324E+03
 .19336E+00   .24627E+02   .75292E+00   .22849E+02   .42047E+01  -.18835E-04   .13573E+01
 .60000E+04   .46920E+01   .15565E+01  -.76998E-05   .48094E+03
 .19220E+00   .24627E+02   .74977E+00   .22842E+02   .41964E+01  -.18835E-04   .13503E+01
 .62000E+04   .46592E+01   .15550E+01  -.77332E-05   .47863E+03
 .19105E+00   .24627E+02   .74661E+00   .22836E+02   .41880E+01  -.18835E-04   .13432E+01
 .64000E+04   .46265E+01   .15534E+01  -.77668E-05   .47632E+03
 .18989E+00   .24627E+02   .74344E+00   .22829E+02   .41796E+01  -.18835E-04   .13362E+01
 .66000E+04   .45938E+01   .15519E+01  -.78009E-05   .47402E+03
 .18873E+00   .24627E+02   .74027E+00   .22823E+02   .41712E+01  -.18835E-04   .13292E+01
 .68000E+04   .45611E+01   .15503E+01  -.78353E-05   .47171E+03
 .18757E+00   .24627E+02   .73708E+00   .22816E+02   .41628E+01  -.18835E-04   .13222E+01
 .70000E+04   .45285E+01   .15487E+01  -.78700E-05   .46941E+03
 .18641E+00   .24627E+02   .73390E+00   .22810E+02   .41543E+01  -.18835E-04   .13152E+01
 .72000E+04   .44959E+01   .15471E+01  -.79051E-05   .46710E+03
 .18525E+00   .24627E+02   .73070E+00   .22803E+02   .41458E+01  -.18835E-04   .13082E+01
 .74000E+04   .44633E+01   .15454E+01  -.79406E-05   .46479E+03
 .18408E+00   .24627E+02   .72750E+00   .22796E+02   .41373E+01  -.18835E-04   .13011E+01
 .76000E+04   .44307E+01   .15440E+01  -.79765E-05   .46249E+03
 .18292E+00   .24627E+02   .72429E+00   .22790E+02   .41287E+01  -.18835E-04   .12941E+01
 .78000E+04   .43982E+01   .15424E+01  -.80128E-05   .46018E+03
 .18176E+00   .24627E+02   .72108E+00   .22783E+02   .41201E+01  -.18835E-04   .12871E+01
 .80000E+04   .43656E+01   .15408E+01  -.80495E-05   .45788E+03
 .18060E+00   .24627E+02   .71785E+00   .22776E+02   .41115E+01  -.18835E-04   .12801E+01
 .82000E+04   .43331E+01   .15391E+01  -.80866E-05   .45557E+03
 .17944E+00   .24627E+02   .71462E+00   .22770E+02   .41028E+01  -.18835E-04   .12730E+01
 .84000E+04   .43006E+01   .15375E+01  -.81240E-05   .45326E+03
 .17828E+00   .24627E+02   .71139E+00   .22763E+02   .40941E+01  -.18835E-04   .12660E+01
 .86000E+04   .42686E+01   .15359E+01  -.81620E-05   .45096E+03
 .17712E+00   .24627E+02   .70814E+00   .22756E+02   .40854E+01  -.18835E-04   .12589E+01
 .88000E+04   .42363E+01   .15343E+01  -.82003E-05   .44865E+03
 .17596E+00   .24627E+02   .70489E+00   .22750E+02   .40767E+01  -.18835E-04   .12519E+01
 .90000E+04   .42040E+01   .15326E+01  -.82391E-05   .44635E+03
.38484E+00
.38191E+01 STOP
```

APPROVAL

ATTITUDE CONTROL AND DRAG COMPENSATION PROPULSION SYSTEM FOR THE GRAVITY PROBE-B SPACECRAFT

by D. H. Blount

The information in this report has been reviewed for technical content. Review of any information concerning Department of Defense or nuclear energy activities or programs has been made by the MSFC Security Classification Officer. This report, in its entirety, has been determined to be unclassified.

A. A. McCool
Director, Structures and Propulsion Laboratory

☆ U.S. GOVERNMENT PRINTING OFFICE: 1983—646-058/163